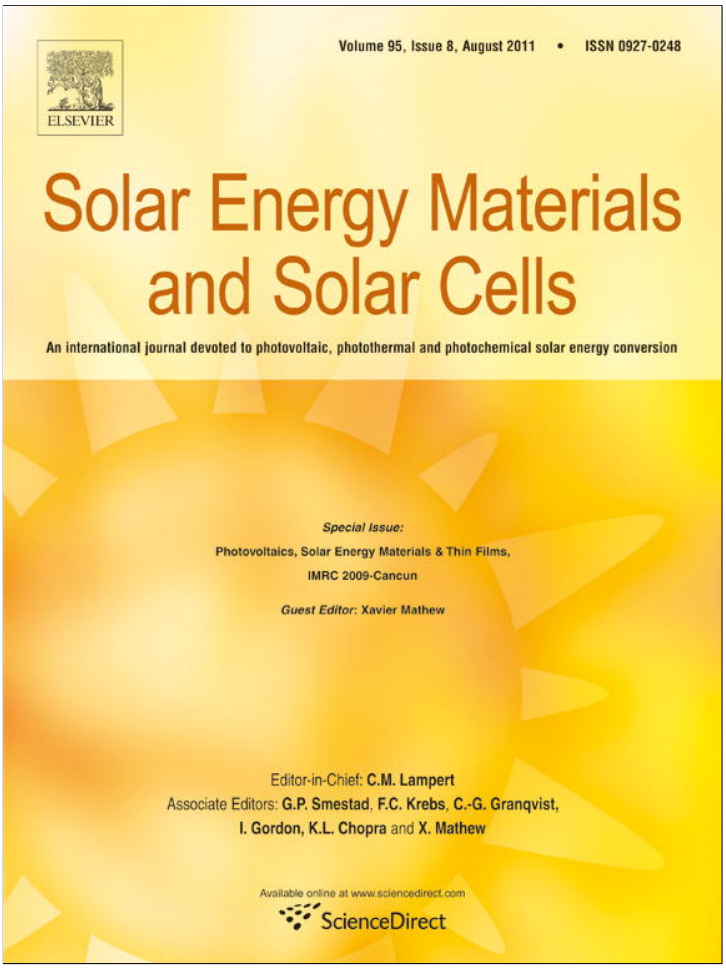

Solar Energy Materials & Solar Cells 95 (2011) 2511–2515

Contents lists available at ScienceDirect

Solar Energy Materials & Solar Cells

journal homepage: www.elsevier.com/locate/solmat

High-efficiency inverted polymer solar cells with solution-processed metal oxides

Yu-Hong Lin [a], Po-Ching Yang [a], Jing-Shun Huang [b], Guo-Dong Huang [c], Ing-Jye Wang [b], Wen-Hao Wu [b], Ming-Yi Lin [b], Wei-Fang Su [c], Ching-Fuh Lin [a,b,*]

[a] Graduate Institute of Electronics Engineering, National Taiwan University, No. 1, Sec. 4, Roosevelt Road, Taipei 10617, Taiwan, ROC
[b] Graduate Institute of Photonics and Optoelectronics, National Taiwan University, No. 1, Sec. 4, Roosevelt Road, Taipei 10617, Taiwan, ROC
[c] Department of Materials Science and Engineering, National Taiwan University, No. 1, Sec. 4, Roosevelt Road, Taipei 10617, Taiwan, ROC

ARTICLE INFO

Article history:
Received 23 February 2011
Received in revised form
28 April 2011
Accepted 3 May 2011
Available online 25 May 2011

Keywords:
Polymer solar cells
Inverted structure
TiO_2 nanorods
Solution-processed

ABSTRACT

The selection of carrier transporting layer in polymer solar cells is an important issue because the nature and direction of carrier transport can be manipulated by inserting different functional layers in the device structure. In this work, we report a very efficient inverted polymer solar cell (PSC) system based on regioregular poly(3-hexylthiophene) and a n-type acceptor, bis-indene[C_{60}]. With a pair of metal oxides and the insertion of TiO_2 nanorods electron collecting layer between the ZnO thin film and the active layer, the device efficiency can be greatly improved. The contact area between the active layer and the electron collecting layer, as well as the thickness of active layer, can be increased with the incorporation of TiO_2 nanorods. As a result, photocurrent can be enhanced due to more absorption of light and more charge separation interface. In addition, the larger contact area and the crystalline TiO_2 nanorods provide a more efficient transporting route for the carriers to the cathode. The most efficient device demonstrated shows a high power conversion efficiency of 5.6% with the inverted structure.

1. Introduction

In recent years, polymer solar cells (PSCs) have emerged as the potential candidate for renewable energy due to the possibility of achieving large area, flexible, and light weight devices with low fabrication cost [1,2]. The bulk-heterojunction PSCs based on regioregular poly(3-hexylthiophene) (rr-P3HT) and fullerene-derivative (6,6)-phenyl C61 butyric acid methyl ester (PCBM) have been reported to reach a power conversion efficiency around 5% [3–5]. The most typical device configuration for this blend system employs an aluminum cathode and a poly(3,4-ethylenedioxythiophene):poly(styrenesulfonate) (PEDOT:PSS)-modified indium–tin oxide (ITO) or fluorine doped tin oxide (FTO) anode. However, PSCs of this conventional configuration suffer from instability problems. The low work function aluminum is easily oxidized in air, and the acidic PEDOT:PSS would degrade the device performance due to the corrosion to indium–tin oxide (ITO), both of which make the device lifetime very short [6–8]. An approach to solve these problems is to use the inverted structure of polymer solar cells by modifying the ITO electrode with an electron selecting layer and replacing the easily oxidized low work function metal electrode by a higher work function one to change the nature of carrier transport [9–12]. Device stability utilizing this inverted configuration can be significantly improved [13–15].

Metal oxides can serve as the transporting functional layer in either cathode or anode. Cathode buffer layers such as zinc oxide (ZnO) [11,16], titanium oxide (TiO_x) [12,17], and cesium carbonate (Cs_2CO_3) [10,18,19] have been reported to possess electron selecting and hole blocking functions, and all of them can be solution-processed. On the other hand, metal oxides such as nickel oxide (NiO) [20], vanadium oxide (V_2O_5) [10], and molybdenum oxide (MoO_3) [16] can function as hole transporting and electron blocking layer in the anode side. However, most of these oxides are deposited by vacuum technique, which is rather expensive and therefore not preferable. To further reduce the fabrication cost, solution-processable anode-side metal oxides layer applicable in polymer solar cells have been developed, such as the sol–gel derived copper oxide (CuO_x) film [21] and the interlayer casted by colloidal dispersion of V_2O_5 and WO_3 [15,22]. These solution-processed metal oxides had been discovered to be able to effectively reduce the device leakage current, thereby improving device characteristics. In addition, because of the easy processing with the solution, many conditions could be quickly experimented for optimization. Finally, by sandwiching the organic layer between these metal oxides, direct

* Corresponding author at: Graduate Institute of Photonics and Optoelectronics, National Taiwan University, Taipei, 10617 Taiwan, ROC. Tel.: +886 2 3366 3540; fax: +886 2 2364 2603.
E-mail address: cflin@cc.ee.ntu.edu.tw (C.-F. Lin).

0927-0248/$ - see front matter © 2011 Elsevier B.V. All rights reserved.
doi:10.1016/j.solmat.2011.05.005

exposure to air can be avoided, resulting in much better device stability.

In this work, we report a very high efficient inverted structure solar cell. It consists of two electron selecting oxide layers, as well as two hole transporting and functional layers, which were all deposited using the solution-process. The ITO electrode is modified by the ZnO sol–gel thin film, and on the top covers the TiO_2 nanorods array. This TiO_2 nanorods layer not only provides larger interfacial area with the organic photoactive blend, but also forms an efficient transporting pathway for electron, thus greatly enhancing the device performance. For hole transport, in addition to the use of solution-processable colloidal suspension of NiO nanoparticles, an additional hole transport ink, developed by Plextronics Inc., is used as the hole transporting layer (HTL) at the anode side. This HTL is based on sulfonated poly(thiophene-3-[2-(2-methoxyethoxy) ethoxy]-2,5-diyl) (S-P3MEET), a stable, inherently doped conjugated polymer. Finally, we demonstrate that inverted PSCs using electronic grade regioregular poly(3-hexylthiophene) and a novel n-type acceptor, bis-indene[C_{60}] (Plexcore® PV2000, Plextronics) [23–26] have high power conversion efficiency of 5.6% with J_{sc}=11.3 mA/cm^2, V_{oc}=0.79 V, and FF=63% under AM 1.5 G (100 mW/cm^2) irradiation intensity when paired with our novel solution-processed metal-oxide interlayer.

2. Experimental

The Plexcore® PV2000 photoactive ink and the Plexcore® hole transport ink (Plexcore® HTL) were provided by Plextronics, Inc. This system has achieved a 5.4%, and later 6.0% power conversion efficiency in conventional device structure and had been certified by National Renewable Energy Laboratory (NREL) [27,28]. The TiO_2 nanorods with diameter of 5 nm and length of 30–40 nm were synthesized by the hydrolysis of titanium tetraisopropoxide as previously reported [29,30]. Nickel(II) oxide nanopowder ($<$50 nm, 99.8%) was purchased from Aldrich and zinc acetate dehydrate was from Sigma-Aldrich. The monoethanolamine (99.5%), the chelating agent and the 2-methoxyethanol (99%), the solvent for sol–gel solution were purchased from Merck and Alfa Aesar, respectively.

The device configuration is shown in Fig. 1. Devices were fabricated on the pre-cleaned ITO coated glass substrate (7 Ω/sq). The ZnO sol–gel thin film (~50 nm) was formed by spin-coating a 0.5 M zinc acetate solution in 2-methoxyethanol and then being annealed at 200 °C for an hour in air. Then TiO_2 nanorods dispersed in pyridine of different concentrations (1.5, 3.0, 3.6, 4.5, and 6.0 mg/ml) were tested and spin-coated onto the ZnO layer at 2000 rpm for 40 s. The samples were heated at 140 °C for 10 min to remove the residual solvent and then transferred into the nitrogen filled glove box. Subsequently, the Plexcore® PV2000 photoactive p/n ink was spin-coated on top of TiO_2 nanorods/ZnO layer at 600 rpm for 40 s and slowly dried in a Petri dish for 30 min. Next, the colloidal suspension of NiO nanoparticles (0.1 mg/ml), which served as both electron blocking and hole conducting layer and then the high-hole-mobility Plexcore® HTL ink, were spin-coated onto the active layer at 2000 and 4000 rpm, respectively. Finally, silver electrode was deposited by thermal evaporation in a vacuum of 2×10^{-6} torr and the device was upon thermal annealing at 170 °C for 10 min in nitrogen atmosphere.

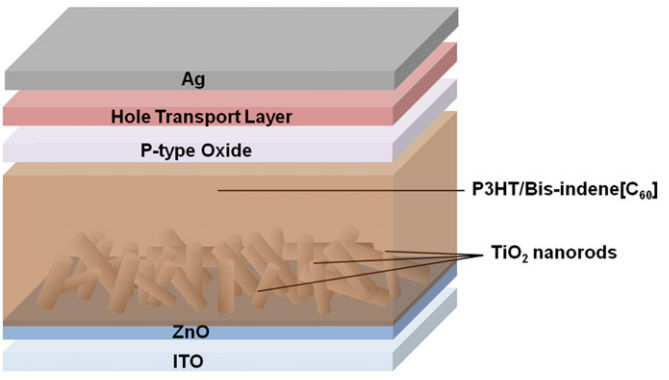

Fig. 1. Schematic diagram of inverted-type device configuration incorporating TiO_2 nanorods as additional electron collecting layer.

The devices were unencapsulated and stored in air. The current density–voltage characteristics were measured with a Keithley 2400 source measurement unit. The solar illumination was generated by a Thermo Oriel 150 W solar simulator with AM 1.5 G filters and calibrated at the intensity of 100 mW/cm^2 by a NREL certificated mono-crystalline silicon reference cell (**PVM-236**). Surface morphology of ZnO layer, together with the TiO_2-nanorods-covered one, was examined by tapping mode atomic force microscopy (NT-MDT Solver P47). A Perkin–Elmer Lambda 35 UV–vis spectrophotometer was used to obtain the device absorption spectra. Field-emission scanning electron microscopy (FESEM) and room temperature photoluminescence spectroscopy (PL) were also applied to analyze device characteristics.

3. Results and discussion

The effects of applying TiO_2 nanorods of different concentration as additional electron collecting network on device performance are investigated. Firstly, all the devices incorporated with TiO_2 nanorods show enhancement of device performance, as shown in Fig. 2. The most apparent improvement of devices lies in V_{oc} (open circuit voltage) and J_{sc} (short circuit current), resulting in substantial improvement in power conversion efficiency (PCE). Secondly, there is an optimal concentration of TiO_2 nanorods. The device fabricated with the 3 mg/ml solution shows the best performance among all the devices, with PCE of 5.6%, V_{oc} of 0.79 V, J_{sc} of 11.3 mA/cm^2, and fill factor (FF) of 63%. As the concentration of TiO_2 solution increased from 1.5 to 3.0 mg/ml, the ZnO surface can be covered more evenly and fully by the nanorods. Therefore, the device performance can be improved. However, when the concentration of TiO_2 nanorods further increases, nanorods start to pile up unevenly onto the ZnO layer, resulting in increase of the contact resistance and thus leading to a lower photocurrent and PCE. To sum up, the above results suggest that adding small amount of TiO2 nanorods between the ZnO and active layer in inverted structure can serve as an effective method to improve the device efficiency, and the details of the device performance are summarized in Table 1. The average value (solid squares) and standard deviation (error bars) of the parameters were derived

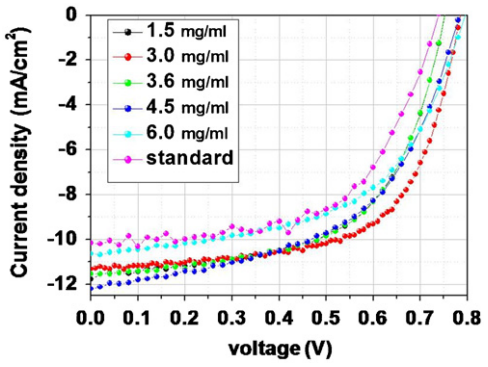

Fig. 2. J–V characteristics of devices with different concentrations of TiO_2 nanorods under 100 mW/cm^2 AM 1.5 G light illumination. All the devices incorporated with TiO_2 nanorods show enhancement of device performance and the optimal concentration of TiO_2 nanorods is 3 mg/ml.

from six individual devices for each TiO_2 concentration, as shown in Fig. 3. All the characterizations followed are with 3 mg/ml TiO_2 nanorods solution in device fabrication.

The atomic force microscopy (AFM) of top surface of ITO/ZnO and ITO/ZnO/TiO_2 nanorods are examined and shown in Fig. 4. In the case of ITO/ZnO, the top surface of ZnO shows a root mean square (RMS) roughness of 7.0 nm and its roughness range is approximately 10 nm; on the other hand, in the case of ITO/ZnO/TiO_2 nanorods the RMS roughness of the top surface becomes 12.6 nm and roughness range is about 40 nm. This greatly increased roughness is attributed to the stacking of TiO_2 nanorods onto the ZnO film, providing a much larger interfacial contact area between the photoactive layer and the inorganic electron collecting layer. The enlarged interfacial area combined with the high mobility of the crystalline TiO_2 nanorods facilitates the electron transporting and collecting. Electron dissociated from the donor/acceptor interface and migrating to the extended inorganic boundary can quickly be collected and channeled to the cathode through the nanorods. These two effects enhance the carrier collection and reduce the series resistance, improving the device characteristics.

Table 1
Summary of device performance with different TiO_2 NRs concentrations.

Concentration (mg/ml)	V_{oc} (V)	J_{sc} (mA/cm^2)	FF (%)	PCE (%)
No TiO_2 NRs	0.74	10.2	58	4.4 ($\pm$0.2)
1.5	0.75	11.8	57	5.1 ($\pm$0.1)
3.0	0.79	11.3	63	5.6 ($\pm$0.1)
3.6	0.78	11.5	57	5.1 ($\pm$0.1)
4.5	0.78	12.1	53	5.0 ($\pm$0.2)
6.0	0.80	10.6	55	4.7 ($\pm$0.2)

Fig. 5(a) shows the absorption spectra of the devices under investigation. The absorption spectrum of glass/ITO/ZnO only device, which barely absorbs light in visible region, was taken as reference. According to the spectra, the device shows an absorption enhancement in the characteristic peaks of semi-crystalline P3HT after incorporating the TiO_2 nanorods. This suggests the thickening of the active layer on the top of nanorods, for the TiO_2 nanorods as-synthesized in this work can only negligibly absorb light of wavelength above 400 nm and therefore will not contribute to absorption, as shown in Fig. 5(a). The cross-sectional FESEM images, as shown in Fig. 5(b), also demonstrate that the active layer thickness of the device has increased from 200 nm (without TiO_2 nanorods) to 280 nm (with TiO_2 nanorods), while the TiO_2 nanorods layer is very thin compared to the active layer. Clearly, the rougher surface can retain more blend solution during the spin-coating process, thus thickening the active layer. However, simply increasing the thickness of active layer cannot improve the device performance. A device without TiO_2 nanorods and with active layer thickness about 280 nm using a spin speed of 500 rpm was also fabricated for reference. Although the J_{sc} of the device is raised to 11.0 mA/cm^2, FF is lowered to 53.4%, leading to a poorer 4.11% power conversion efficiency. This phenomenon is related to the limitation of active layer thickness imposed by the insufficient carrier mobility in organic film. A thicker organic film results in an increased series resistance, which derives from the increased charge recombination, and therefore degrades the device performance. The above result shows that the device efficiency cannot be improved solely by the thickening of active layer without adding TiO_2 nanorods.

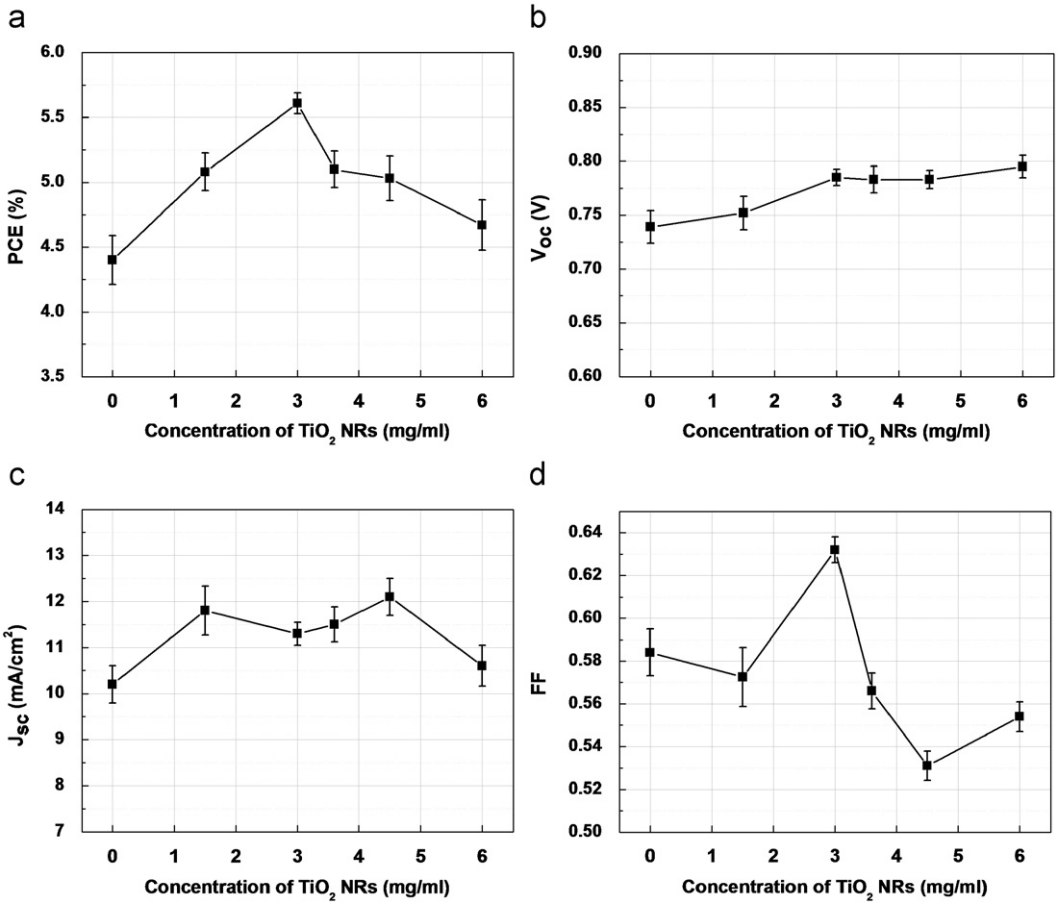

Fig. 3. Photovoltaic parameters of devices with error bars (standard deviation) for (a) PCE, (b) V_{oc}, (c) J_{sc}, and (d) FF.

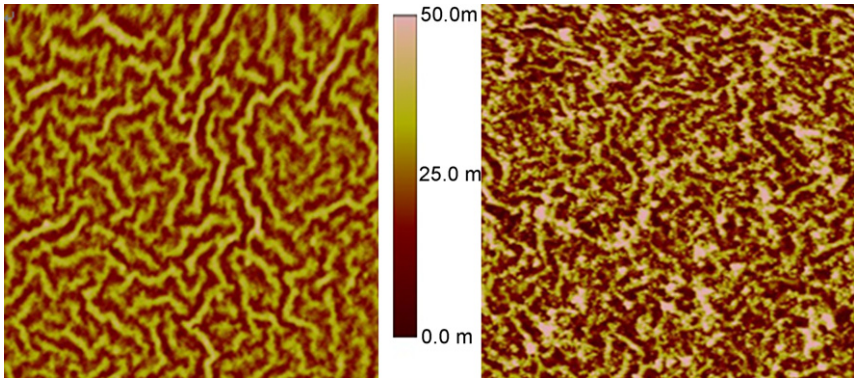

Fig. 4. AFM images of the top surface of ITO/ZnO (left) and ITO/ZnO/TiO_2 NRs (right). AFM image scans are 5 μm × 5 μm.

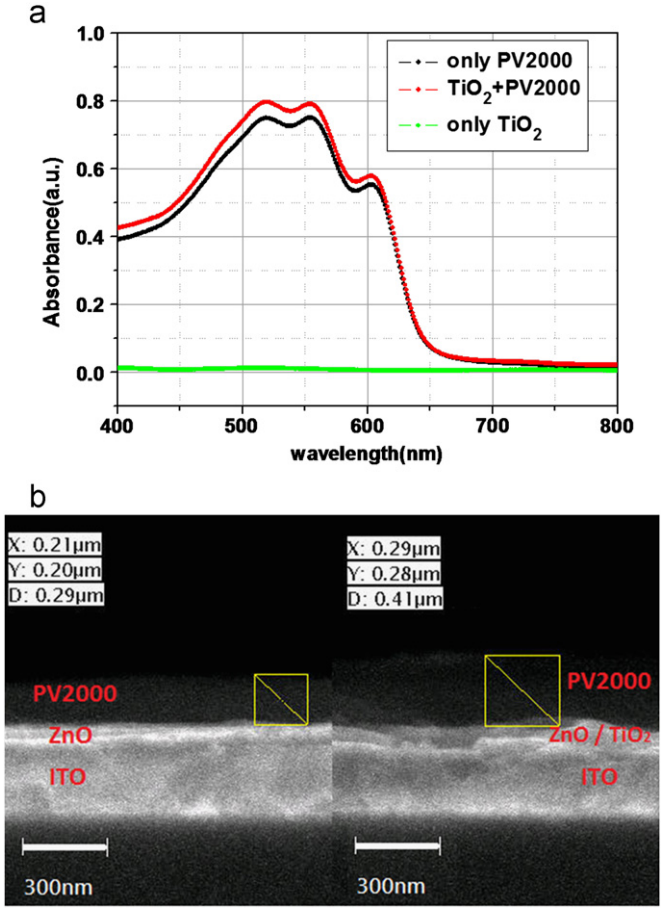

Fig. 5. (a) Absorption spectra of the devices with and without the TiO_2 nanorods, where glass/ITO/ZnO only device is taken as reference. After incorporating the TiO_2 nanorods, the device shows an absorption enhancement in the characteristic peaks of semi-crystalline P3HT. (b) FESEM cross-sectional images of the devices without (left) and with (right) TiO_2 nanorods.

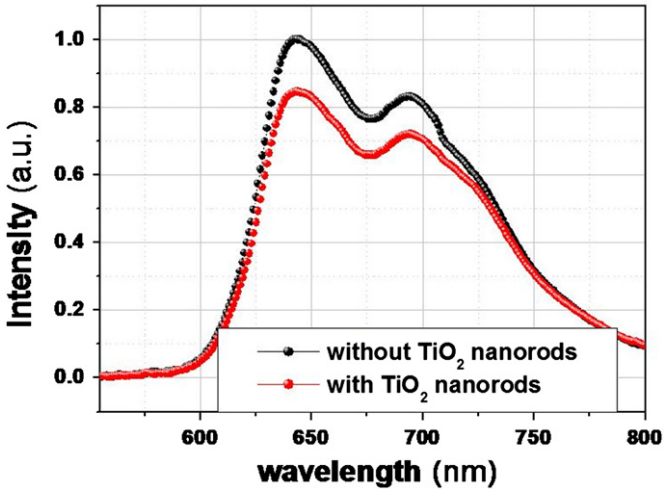

Fig. 6. Room temperature photoluminescence spectra of the devices. The PL quenching effect indicates that the TiO_2 nanorods facilitates the charge separation process.

There is another possible reason that accounts for the performance enhancement of the device after adding TiO_2 nanorods. In the regime of organic/inorganic hybrid solar cells, P3HT/TiO_2 heterojunction system has been reported to have efficiencies above 2% [31], where the organic P3HT acts as the donor material and the inorganic TiO_2 serves as the acceptor material. In our device configuration, the TiO_2 nanorods/P3HT interface can also contribute additional photocurrent to the solar cell. This can be clearly seen from the room temperature PL spectra of the devices with and without TiO_2 nanorods, as shown in Fig. 6. From the figure, the photoluminescence intensity of TiO_2 nanorods incorporated device is significantly lowered compared to the one without TiO_2. This so-called PL quenching evidently indicates that TiO_2 nanorods could provide additional charge separating interface at its boundary with P3HT/bis-indene[C_{60}] blend, thereby improving the device performance.

Finally, device stability has been examined. The devices were not encapsulated and have been tested periodically for 500 h. A control device with configuration ITO/ZnO/PV2000/Ag has also been examined. After 500 h storage in air, the control device PCE has declined from 3.2% to 1.0%, about a 70% degradation. In contrast, the device incorporating the solution-processed NiO layer and the hole transporting layer decays much slower, with only a 23% degradation (4.4%–3.4%). In addition, the devices with and without TiO_2 nanorods show almost the same stability that all the devices can retain about 75% of the device efficiency after 500 h storage. These results imply that the stability improvement is attributed to the anode-side interfacial layers, which is similar to our previous report based on the P3HT/PCBM system [15]. The metal oxide and the S-P3MEET layer can serve as a barrier against water and oxygen, and therefore protect the active layer from oxidation, improving the device stability.

4. Conclusions

In conclusion, we have demonstrated the use TiO_2 nanorods as the additional electron collecting layer in the inverted structure

PSCs. TiO_2 nanorods can enlarge the interfacial contact area and play a role in the charge separation process with P3HT. In addition, devices incorporating TiO_2 nanorods can sustain thicker active layer without sacrificing the fill factor, therefore enhancing light absorption and device efficiency. The device stability has also been tested and found to be much superior to the control device without anodic modification. The most efficient device based on the P3HT/bis-indene[C_{60}] system and TiO_2 nanorods shows the PCE of 5.6% using the commercially available high-performance photoactive ink system.

Acknowledgment

This work was supported by the National Science Council, Taiwan, Republic of China. The NSC nos. are NSC99-2221-E-002-104-MY3 and NSC97-2221-E-002-039-MY3.

References

[1] F.C. Krebs, Fabrication and processing of polymer solar cells: a review of printing and coating techniques, Sol. Energy Mater. Sol. Cells 93 (2009) 394–412.
[2] C.J. Brabec, J.R. Durrant, Solution-processed organic solar cells, MRS Bull. 33 (2008) 670–675.
[3] G. Li, V. Shrotriya, J. Huang, Y. Yao, T. Moriarty, K. Emery, Y. Yang, High-efficiency solution processable polymer photovoltaic cells by self-organization of polymer blends, Nat. Mater. 4 (2005) 864–868.
[4] W. Ma, C. Yang, X. Gong, K. Lee, A.J. Heeger, Thermally stable, efficient polymer solar cells with nanoscale control of the interpenetrating network morphology, Adv. Funct. Mater. 15 (2005) 1617–1622.
[5] A.J. Moulé, K. Meerholz, Controlling morphology in polymer-fullerene mixtures, Adv. Mater. 20 (2008) 240–245.
[6] M. Jørgensen, K. Norrman, F.C. Krebs, Stability/degradation of polymer solar cells, Sol. Energy Mater. Sol. Cells 92 (2008) 686–714.
[7] M.P. de Jong, L.J. van IJzendoorn, M.J.A. de Voigt, Stability of the interface between indium–tin oxide and poly(3,4-ethylenedioxythiophene)/poly(styrenesulfonate) in polymer light-emitting diodes, Appl. Phys. Lett. 77 (2000) 2255–2257.
[8] K.W. Wong, H.L. Yip, Y. Luo, K.Y. Wong, W.M. Lau, K.H. Low, H.F. Chow, Z.Q. Gao, W.L. Yeung, C.C. Chang, Blocking reactions between indium–tin oxide and poly(3,4-ethylene dioxythiophene):poly(styrenesulphonate) with a self-assembly monolayer, Appl. Phys. Lett. 80 (2002) 2788–2790.
[9] Y. Şahin, S. Alem, R. de Bettignies, J.-M. Nunzi, Development of air stable polymer solar cells using an inverted gold on top anode structure, Thin Solid Films 476 (2005) 340–343.
[10] G. Li, C.-W. Chu, V. Shrotriya, J. Huang, Y. Yang, Efficient inverted polymer solar cells, Appl. Phys. Lett. 88 (2006) 253503-1–253503-3.
[11] M.S. White, D.C. Olson, S.E. Shaheen, N. Kopidakis, D.S. Ginley, Inverted bulk-heterojunction organic photovoltaic device using a solution-derived ZnO underlayer, Appl. Phys. Lett. 89 (2006) 143517-1–143517-3.
[12] C. Waldauf, M. Morana, P. Denk, P. Schilinsky, K. Coakley, S.A. Choulis, C.J. Brabec, Highly efficient inverted organic photovoltaics using solution based titanium oxide as electron selective contact, Appl. Phys. Lett. 89 (2006) 233517-1–233517-3.
[13] F.C. Krebs, Air stable polymer photovoltaics based on a process free from vacuum steps and fullerenes, Sol. Energy Mater. Sol. Cells 92 (2008) 715–726.
[14] L.M. Chen, Z. Hong, G. Li, Y. Yang, Recent progress in polymer solar cells: manipulation of polymer:fullerene morphology and the formation of efficient inverted polymer solar cells, Adv. Mater. 21 (2009) 1434–1449.
[15] J.S. Huang, C.Y. Chou, C.F. Lin, Efficient and air-stable polymer photovoltaic devices with WO_3–V_2O_5 mixed oxides as anodic modification, IEEE Electron Device Lett. 31 (2010) 332–334.
[16] A.K.K. Kyaw, X.W. Sun, C.Y. Jiang, G.Q. Lo, D.W. Zhao, D.L. Kwong, An inverted organic solar cell employing a sol–gel derived ZnO electron selective layer and thermal evaporated MoO_3 hole selective layer, Appl. Phys. Lett. 93 (2008) 221107-1–221107-3.
[17] C.Y. Li, T.C. Wen, T.H. Lee, T.F. Guo, J.C.A. Huang, Y.C. Lin, Y.J. Hsu, An inverted polymer photovoltaic cell with increased air stability obtained by employing novel hole/electron collecting layers, J. Mater. Chem. 19 (2009) 1643–1647.
[18] J. Huang, G. Li, E. Wu, Q. Xu, Y. Yang, Achieving high-efficiency polymer white-light-emitting devices, Adv. Mater. 18 (2006) 114–117.
[19] H.H. Liao, L.M. Chen, Z. Xu, G. Li, Y. Yang, Highly efficient inverted polymer solar cell by low temperature annealing of Cs_2CO_3 interlayer, Appl. Phys. Lett. 92 (2008) 173303-1–173303-3.
[20] M.D. Irwin, D.B. Buchholz, A.W. Hains, R.P.H. Chang, T.J. Marks, p-Type semiconducting nickel oxide as an efficiency-enhancing anode interfacial layer in polymer bulk-heterojunction solar cells, Proc. Natl. Acad. Sci. USA 105 (2008) 2783–2787.
[21] M.Y. Lin, C.Y. Lee, S.C. Shiu, I.J. Wang, J.Y. Sun, W.H. Wu, Y.H. Lin, J.S. Huang, C.F. Lin, Sol–gel processed CuO_x thin film as an anode interlayer for inverted polymer solar cells, Org. Electron. 11 (2010) 1828–1834.
[22] J.S. Huang, C.Y. Chou, M.Y. Liu, K.H. Tsai, W.H. Lin, C.F. Lin, Solution-processed vanadium oxide as an anode interlayer for inverted polymer solar cells hybridized with ZnO nanorods, Org. Electron. 10 (2009) 1060–1065.
[23] R.D. McCullough, R.S. Loewe, Method of forming poly-(3-substituted) thiophenes, US Patent 6,166,172 A, December 26, 2000.
[24] D.W. Laird, R. Stegamat, M. Daadi, H. Richter, V. Vejins, L. Scott, T.A. Lada, Organic photovoltaic devices comprising fullerenes and derivatives thereof, US Patent Application Publication No. US 2010/0132782 A1, June 3, 2010.
[25] Y. He, H.-Y. Chen, J. Hou, Y. Li, Indene-C_{60} bisadduct: a new acceptor for high-performance polymer solar cells, J. Am. Chem. Soc. 132 (2010) 1377–1382.
[26] G. Zhao, Y. He, Y. Li, 6.5% efficiency of polymer solar cells based on poly(3-hexylthiophene) and indene-C_{60} bisadduct by device optimization, Adv. Mater. 22 (2010) 4355–4358.
[27] M.A. Green, K. Emery, Y. Hishikawa, W. Warta, Solar cell efficiency tables (version 31), Prog. Photovoltaics 16 (2008) 61–67.
[28] M.A. Green, K. Emery, Y. Hishikawa, W. Warta, Solar cell efficiency tables (version 34), Prog. Photovoltaics 17 (2009) 320–326.
[29] T.W. Zheng, Y.Y. Lin, H.H. Lo, C.W. Chen, C.H. Chen, S.C. Liou, H.Y. Huang, W.F. Su, A large interconnecting network within hybrid MEH-PPV/TiO_2 nanorod photovoltaic devices, Nanotechnology 17 (2006) 5387–5392.
[30] P.D. Cozzoli, A. Kornowski, H. Weller, Low-temperature synthesis of soluble and processable organic-capped anatase TiO_2 nanorods, J. Am. Chem. Soc. 125 (2003) 14539–14548.
[31] Y.Y. Lin, T.H. Chu, S.S. Li, C.H. Chuang, C.H. Chang, W.F. Su, C.P. Chang, M.W. Chu, C.W. Chen, Interfacial nanostructuring on the performance of polymer/TiO_2 nanorod bulk heterojunction solar cells, J. Am. Chem. Soc. 131 (2009) 3644–3649.